DOI: 10.18721/JPM.13107
УДК 621.455.4; 621.455.34

# THE CONTACT IONIZATION ION ACCELERATOR FOR THE ELECTRICALLY POWERED SPACECRAFT PROPULSION: A COMPUTER MODEL

*D.B. Dyubo, O.Yu. Tsybin*

Peter the Great St. Petersburg Polytechnic University, St. Petersburg, Russian Federation

An analytical electrodynamic algorithm has been developed in order to study physical processes and calculate mechanical forces in an ion accelerator. This algorithm is combined with computer simulation of the electromagnetic field and charged particles' trajectories. Computer models of ion accelerators with surface or contact ionization in the injection region were considered as an example. Ultimately, the created theoretical apparatus makes it possible to evaluate the proposed engineering solutions and diagnostic parameters of electric spacecraft propulsions as well as to compare the applicability of various working agents inside.

**Keywords:** computer modeling, ionization, ion beam, ion accelerator, electrically powered spacecraft propulsion

**Citation:** Dyubo D.B., Tsybin O.Y., The contact ionization ion accelerator for the electrically powered spacecraft propulsion: a computer model, St. Petersburg Polytechnical State University Journal. Physics and Mathematics. 13 (1) (2020) 73–84. DOI: 10.18721/JPM.13107



# КОМПЬЮТЕРНАЯ МОДЕЛЬ УСКОРИТЕЛЯ ИОНОВ С КОНТАКТНОЙ ИОНИЗАЦИЕЙ ДЛЯ ЭЛЕКТРОРАКЕТНЫХ ДВИГАТЕЛЕЙ КОСМИЧЕСКИХ ЛЕТАТЕЛЬНЫХ АППАРАТОВ

*Д.Б. Дюбо, О.Ю. Цыбин*

Санкт-Петербургский политехнический университет Петра Великого,

Санкт-Петербург, Российская Федерация

С целью исследования физических процессов и расчета механических сил в ускорителе ионов, построен аналитический электродинамический алгоритм, объединенный с компьютерным моделированием электромагнитного поля и траекторий заряженных частиц. В качестве примера рассмотрены компьютерные модели ускорителей ионов с поверхностной или контактной ионизацией в области инжекции. Созданный теоретический аппарат позволит оценивать предполагаемые конструкторские решения и параметры разрабатываемых электроракетных двигателей космических летательных аппаратов, сравнивать применение в них различных рабочих веществ.

**Ключевые слова:** компьютерное моделирование, ионизация, ионный поток, ионный ускоритель, электроракетный двигатель

**Ссылка при цитировании:** Дюбо Д.Б., Цыбин О.Ю. Компьютерная модель ускорителя ионов с контактной ионизацией для электроракетных двигателей космических летательных аппаратов // Научно-технические ведомости СПбГПУ. Физико-математические науки. 2020. Т. 13. № 1. С. 78–91. DOI: 10.18721/JPM.13107

## Introduction

Accelerated ion fluxes in vacuum are widely used in research, medicine, materials science, microelectronics, as well as in technologies for thin film deposition, surface cleaning, etc. [1–5]. Ion accelerators have gained great importance for spacecraft technologies, particularly for electric propulsion spacecraft [6–9]. Fundamental research in this field [10–14] yielded significant results, laying the foundation for theoretical studies [15–19] and computer simulation methods [17–19].

Typical electric propulsion systems are vacuum ion and plasma ion devices converting electromagnetic energy generated by accelerating ions of the propellant into mechanical energy accelerating the spacecraft. Two types of electric propulsion accelerators are commonly used: ion and plasma ion [6, 10, 11]. Electric propulsion encompasses a wide range of complex phenomena, including conversion of the propellant into the vapor-gas phase, ionization, characteristics of plasma in the ionization chamber, injection of plasma and ions into the accelerator and their acceleration, mechanical forces arising and their parameters, beam neutralization, charge exchange, extraction and positioning. Fast ions leaving the accelerator should be neutralized to prevent charging of the spacecraft body, the associated drop in thrust, and secondary discharge phenomena. The beam of neutralized particles is ejected outwards at high velocities, up to tens of km/s, which is much higher than in chemical jet engines. Modern electric propulsion systems mainly use compressed gases, particularly xenon, as propellants. However, xenon is a rare and expensive gas, so efforts are underway to find alternatives for large-scale projects of electric propulsion engines. Electric propulsion engines based on novel methods and technologies should combine simple, reliable and durable design with affordable costs, running on alternative types of propellants, effectively generating the required thrust with reduced consumption of the reactant mass [8, 12–14]. Perfecting the theory and methods for analysis of ionic and mechanical processes in accelerators, as well as conducting flight and ground experiments can establish an effective framework for constructing new electric propulsion systems. Bench tests are run in ground laboratories, typically with large and expensive vacuum systems, taking longer time to operate and consuming considerable amounts of propellants.

Analytical methods are mainly used in theory of electric propulsion for the most simple ion optical and electrodynamic problems [10–15]. Effective solutions for plasma states are obtained by numerically simulating the dynamics of enlarged particles by time steps (the Monte Carlo method) [17–19]. Differential equations in finite-difference form, grid methods, and Fourier transforms are used for simulations of electromagnetic fields and particle trajectories in these fields. However, this classic method is rather complicated, requiring a lot of computer time. The CST Studio Suite for three-dimensional modeling developed by Computer Simulation Technology is an effective tool for trajectory analysis of different electron and ion devices taking into account the intrinsic electric field of the space charge [20, 21]. However, no known studies have reported on applying CST codes to analysis or design of ion or plasma ion electric propulsion systems. While microscopic power characteristics are crucially important, insufficient attention has been given to electrodynamic models and simulations of mechanical processes in accelerators, hindering the progress in new devices. The dependences of thrust on coordinates, shape of electrodes, operating modes of the reactor, and other parameters are not described in known literature. It is usually accepted for simplicity, regardless of structural elements, that the thrust can be expressed in terms of beam parameters

$$F_f = v_{in}(dm_w/dt),$$

where $dm_w/dt$ is the mass flux $m_w$ of propellant in the neutralized beam, $t$ is the time; $v_{in}$ is the velocity of a neutral particle in the beam.

At the same time, the values of $dm_w/dt$ are not measured. The resulting thrust $F_f$ of electrostatic ion and plasma ion engines is formulated in terms of current $I$ and voltage $U_d$ for ions with the mass μ and charge $q$ in the accelerating gap (see, for example, [10, 11]):

$$F_f = I[2U_d(\mu/q)]^{1/2}.$$

It is assumed that the ion field at the output of the accelerator is equal to zero, flux and velocity of particles in the beam are equal to the same values in the accelerator and do not change in the neutralizer; neutralization has 100% efficiency, there are no oppositely charged particles in the acceleration chamber, ions have no transverse velocity components, there are no losses, collisions and charge exchange of ions, etc.

This simplification produces inaccuracies in accounting for the ion-optical properties of the injector, accelerator, and neutralizer, as well as for the microscopic processes associated with generation of mechanical forces. Essentially, the accuracy of the above formulas requires further assessment.

Like the Monte Carlo method and some other similar modeling packages, the CST package is inapplicable to detecting the relationships between mechanical forces in ion accelerators and internal microscopic processes.

The goal of this study consists in constructing an electrodynamic algorithm for determining mechanical parameters, combined with computer simulation in the CST Suite to establish the above-mentioned relationships. Furthermore, our practical task was to apply the developed tools to studying physical processes in ion and plasma ion electric propulsion systems.

## Electrodynamic algorithm for determining the mechanical parameters of ion and plasma ion accelerators

The CST model combined with the electrodynamic algorithm was primarily used to analyze ion trajectories in inhomogeneous fields generated by single-stage and multi-stage DC accelerators, taking into account polarization charges and the space charge formed by the charged particle flux. As a result of analysis, we proposed an electrodynamic algorithm accounting for the relationship of mechanical properties with structural elements and modes, characteristics of the main processes and propellants. The algorithm consists of interconnected modules of varying complexity, allowing to simulate both simple elements of the accelerator and their combinations.

The algorithm for determining the mechanical parameters of electrostatic acceleration of ions is based on the following principles.

In combination, the accelerating voltage applied and space charges in the accelerator induce certain polarization charges. These are surface charges bound on electrodes and distributed over their surfaces; the distribution depends on the geometric shape, size and arrangement of the electrodes.

The momentum for engine thrust is generated in the ion acceleration chamber. The thrust applied to the electrodes arises due to Coulomb attraction of surface polarization charges to accelerated ions. The main condition and process for generating mechanical thrust is acceleration of ions by an electric field in the accelerator, their subsequent neutralization and ejection of a beam of neutral particles into space. Accelerated ions should be neutralized because the ions escaping generate an excess charge of the opposite sign. Such a charge inhibits the escaping ions, reducing the thrust, and also causes destructive discharge phenomena in the structural elements of the device. The action of the force $F_{TM}$ produces mechanical stress in the mount of the device fixed on the test bench; the action of this force provides acceleration of the flying spacecraft.

A simplified diagram of a typical single-stage DC ion accelerator for an electric propulsion engine of spacecraft is shown in Fig. 1.

Fig. 1 shows space charge *3* of internal ions with the total mass $m$ and velocity $v(z)$ in the accelerator; beam *5* of neutralized particles is ejected outwards at velocity $v_f$. The force $F_{Ti}$ acting on the ion flux from bound surface charges *2* is equal to the inertia of the ions with mass $m$:

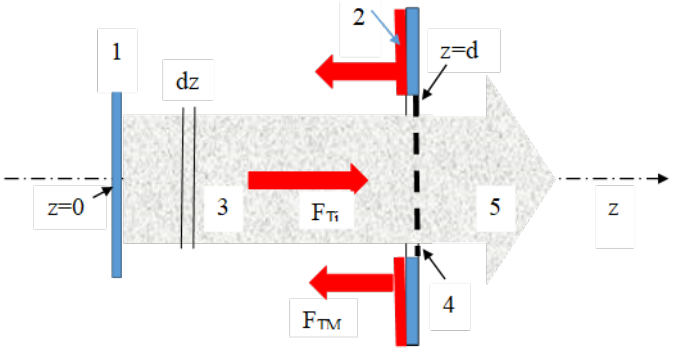


Fig. 1. Simplified diagram of single-stage ion accelerator:
input electrode *1* in ion injection plane ($z = 0$); bound charges *2* on output electrode in ion extraction plane ($z = d$); space charge *Q 3*; ion neutralization region *4*; beam *5* of neutralized particles ejected outwards; $F_{TM}$, $F_{Ti}$ are the forces acting on the output electrode from the ion flux and on the ion flux from the bound charges, respectively

$$F_{Ti} = m(dv/dt).$$

The force $F_{TM}$ acting on the output electrode from ion flux *3* is expressed as

$$F_{TM} = -v(dm/dt).$$

Ion acceleration is generated by attraction to surface charges, which is calculated as the Lorentz force acting on charged particles from the electric field in the accelerator, taking into account the polarization charges of electrodes. Notably, the parameters of ion flux in the above two formulas refer to the particles in the accelerator rather than the beam.

Ion drift in the accelerating gap is directed along the $z$ axis from injection plane *1* with $z = 0$ to neutralization plane *4*. Instantaneous internal charge and mass in the accelerating gap are equal to $Q$ and $m$, gap width is equal to $d$.

Modern plasma ion or Hall-effect thrusters generate propellant plasma directly in the accelerating gap combined with the ionization chamber, while ion thrusters generate propellant plasma in the volume chamber to the left of the injection plane (see Fig. 1), subsequently extracting the ions into the accelerating gap by the electric field.

**Processes in the accelerating gap.** Acceleration of ions by the force $F_{Ti}$ along the axis $z$ balances the inertia of the accelerated spacecraft in the center of mass and ends with beam ejection. Ions attract the electrode with induced charges bound to it it with the force $F_{TM}$, resulting in reverse acceleration of spacecraft's center of mass in the direction opposite to the $z$ axis (see Fig. 1). Accordingly, the thrust $F_{TM}$ accelerating the spacecraft is generated only by the ions in the gap and should become zero when the ions pass through the plane of the exit gap and the neutralization region, if the latter coincides with plane *4* (see Fig. 1).

Using the kinetic (mechanical) approach, we obtain the force $F_{Ti}$ by integrating the inertia along the ion acceleration path:

$$F_{Ti}(z) = \int_0^z \frac{dv(z)}{dt} dm(z), \qquad (1)$$

where $dm(z)$ is the mass of each layer $dz$, $v(z)$ is the velocity of this layer.

Electrodynamically, this force can be calculated as a set of Lorentz forces acting from the electric field $E$ on the charge $dQ(z)$ in each layer $dz$:

$$F_{Ti}(z) = \int_0^z E(z)\, dQ(z). \qquad (2)$$

Naturally, the forces calculated by Eqs. (1) and (2) should coincide for a given value of the coordinate $z$, including with $z = d$.

To tentatively test the algorithm and the computer program, we determined the values of the physical quantities included in Eqs. (1) and (2) based on simple models, using, for example, a plane-parallel gap with solid electrodes. The ion current in such an accelerating gap is determined analytically by the Child–Langmuir formula in saturation mode, i.e., with space-charge limited current (SCLC). Accordingly, ions are injected into into the accelerator at zero electric field and with a zero initial velocity. Since the field is zero, the charge on the input surface is zero, and the polarization charge $Q_p$, equal in magnitude to the internal drift charge $Q$ in magnitude but opposite in sign, is concentrated on the inner surface of the solid output electrode. Well-known formulas include the dependence of current $I$ on voltage $U_d$ according to the three halves power law, distributions of potential $U(z)$, ion velocity $v(z)$, electric field $E(z)$, as well as the total thrust, charge and mass of ions in the gap [1, 2, 10, 15, 16]:

$$I = \frac{4}{9}\sqrt{2\frac{q}{\mu}}\varepsilon_0 S U_d^{\frac{3}{2}} d^{-2},$$

$$E(z) = \frac{4}{3} U_d d^{-\frac{4}{3}} z^{\frac{1}{3}},$$

$$E_0 = \frac{U_d}{d}, E_d = \frac{4}{3} E_0,$$

$$F_i = \frac{1}{2}\varepsilon_0 S E_d^2 = \frac{8}{9}\varepsilon_0 S E_0^2,$$

$$Q = \frac{4}{3}\varepsilon_0 S E_0, m = \frac{\mu}{q} Q.$$

The following notations are used here: $S$ is the cross-sectional area of the gap; μ is the ion mass; $q$ is the ion charge; $\varepsilon_0$ is the electric constant ($\varepsilon_0 \approx 8.85 \cdot 10^{-12}$ F/m).

Developing this well-known model, we obtain new distributions along the $z$ coordinate for thrust, charge and mass of a thin layer $dz$ inside the accelerating gap:

$$dF_{Ti}(z) = \frac{16}{27}\varepsilon_0 S E_0^2 d^{-\frac{2}{3}} z^{-\frac{1}{3}} dz,$$
$$dQ(z) = \frac{4}{9}\varepsilon_0 S U_d d^{-\frac{4}{3}} z^{-\frac{2}{3}} dz. \qquad (3)$$

Relations (3) describe the mechanical field of velocities and the distribution of propellant masses in the accelerator. The values of the physical quantities satisfy the system of Poisson's equations, equations of motion and continuity (for the given boundary and initial conditions) in the accelerator in quasistatic, nonrelativistic, non-diamagnetic collisionless hydrodynamic approximations. Descriptions of Lorentz and Coulomb forces in the accelerator are related by the Gauss law. For example, the distribution of charge (see Eq. (3)) and electric field $E(z)$ is consistent with the Gauss theorem for each thin layer $dz$ and for the entire gap as a whole. Eqs. (2) and (3) imply the dependence of the force acting on the ions in SCLC mode from zero to the $z$ coordinate in the gap:

$$F_{Ti}(z) = \frac{8}{9}\varepsilon_0 S E_0^2 \left(\frac{z}{d}\right)^{\frac{2}{3}}. \qquad (4)$$

Accordingly, the kinetic power $W_i$ of ion flux (in the spacecraft's own reference frame) is equal to the electric power supplied to the accelerator (excluding heat losses):

$$W_i = \int_0^d v(z) E(z) dQ(z) = \\ = \frac{4}{9}\varepsilon_0 S E_0^2 v(d) = IU_d. \qquad (5)$$

Therefore, the ratio of thrust to input power in the model of a solid output electrode reaches its maximum value and is determined by the formula

$$F_{TM}/W_i = \beta/v(d);\ \beta = 2. \qquad (6)$$

However, the electric field in the gap decreases depending on the shape of the partially open output electrode (grid, aperture, notch, etc.), and the coefficient $\beta < 2$ as a result. According to Eqs. (1)–(6), the mechanical parameters of a complex multi-stage DC accelerator can be calculated by obtaining the spatial distributions of electric field $E(z)$, charge $Q(z)$ and velocity $v(z)$ of ions, taking into account polarization charges and space charge, which can be determined by computer simulation. Computer monitors collecting data on microscopic processes were installed in the region of ion and electron fluxes for these purposes.

Microscopic parameters of trajectories and characteristics of physical processes were obtained for the first time, including distributions depending on the coordinate $z$ along the spacecraft axis: particle velocities, fields $E(z)$ and potentials, charges $dQ(z)$ and currents, taking into account the intrinsic electric field of space charge of ions and electrons.

A more complicated physical process was considered at the next stage; we analyzed the neutralization of the ion flux by injecting an electron beam into this flux.

### Testing of two, three and multi-electrode ion accelerators

To verify the calculations, we first simulated and tested a simple planar two-electrode model whose sizes and modes were tailored to closely match the one-dimensional model in SCLC mode. The technique was verified by comparing it with analytical calculations using Eqs. (1)–(6). We additionally tested well-known designs based on Pierce gun algorithms [5, 16].

The three, four, five and six-electrode models were implemented at the second stage. We used a partitioned set of nonplanar electrodes to impose inhomogeneous boundary conditions compensating for the difference between Laplace and Poisson fields at the boundaries. The surfaces for injection into the accelerating gap were given as both smooth planar and smooth parabolic. We simulated emission of ions with different specific charges in SCLC mode in this configuration. In practice, this meant that surface-contact ionization [22–25] was simulated; its prospects for use in ion and plasma ion accelerators are estimated to be better than those of surface-volume ionization [26, 27].

Ion trajectories were constructed for all models considered (partially shown below as examples); microscopic parameters were collected using computer monitors for these trajectories. The surfaces of the boundary parallelepiped surrounding the entire structure were sufficiently far from the accelerating gaps, with a fixed zero potential maintained.

**Example calculations** Typical dependences of electronic, physical and mechanical parameters on coordinates and operating modes for models of ion accelerators using xenon ions are shown in Figs. 2–6.

The following parameters of two-electrode models were chosen for the examples:

voltage $U_d$ between the plates up to 2 kV,
ion flux diameter 20 mm,
distance between the plates $d$ = 4 mm,
emission area $S$ = 314 mm$^2$.

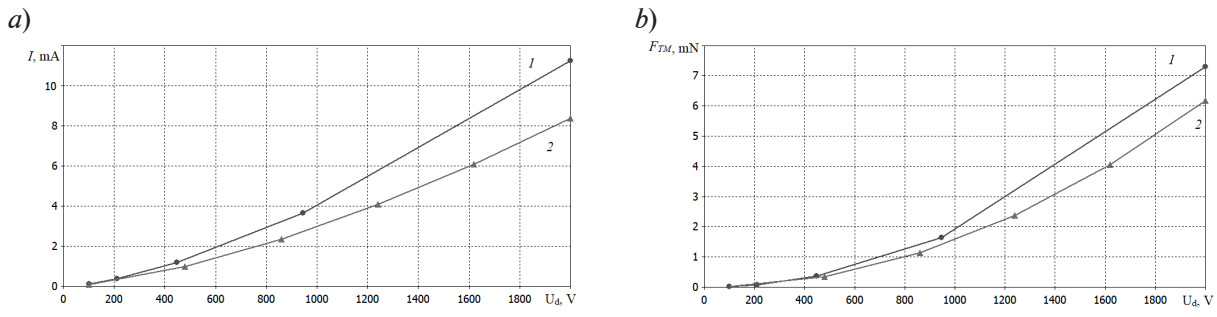


Fig. 2. Numerical (*1*) and analytical (*2*) calculations of current (*a*) and resultant mechanical force (*b*) as functions of voltage $U_d$ between the plates. A two-electrode model A with xenon ions ($d$ = 4 mm) was used

The calculations were carried out for three models:

Model A with two solid electrodes;

model G (grid) with one solid and one grid electrode;

models D5 and D10 with one solid and one grid electrodes, with apertures 5 mm (D5) and 10 mm (D10) in diameter.

The figures show the characteristics obtained by analytical (for SCLC mode) and numerical calculations.

The numerical results are close to theoretical analytical curves with the largest deviation of about 10%. This discrepancy can be explained, firstly, by edge effects due to finite sizes and open boundaries of the accelerating gap, and secondly, by errors in calculating the field and particle velocity near the boundary $z = 0$ in the computer model. Introducing corrections reduced the discrepancy between analytical and computer parameters to 1% or less. The results obtained allowed to consider more complex multi-electrode structures of ion thrusters.

The simple three-electrode 2D models we tested were fundamentally close to real electric propulsion systems constructed for spacecraft. Typical electric propulsion systems use volume ionization in a chamber limited by a grid with multiple apertures [6, 10, 11]. A grid or a solid electrode with an aperture which was an electrostatic focusing lens was placed between

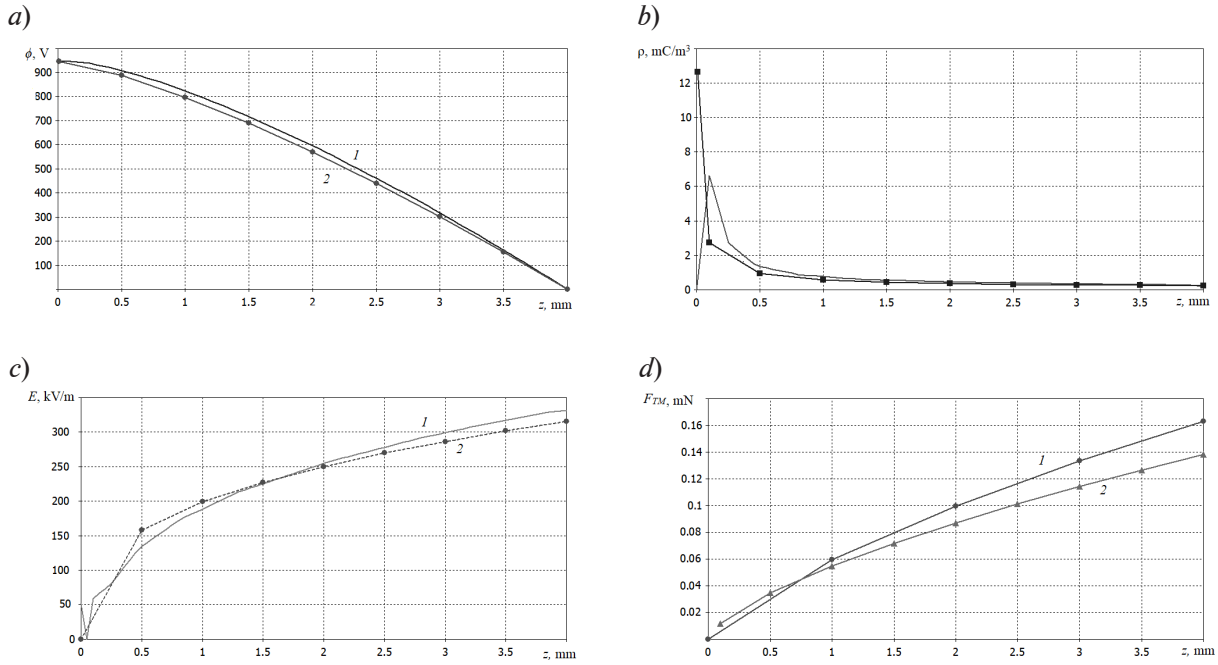


Fig. 3. Numerical (*1*) and analytical (*2*) calculations for distributions of potential (*a*), space charge density (*b*), electric field (*c*) and resultant mechanical force $F_{TM}$ (*d*) along coordinate $z$ along the central axis of ion accelerator. A two-electrode model A with xenon ions ($d$ = 4 mm) was used; $U_d$ = 945.74 V

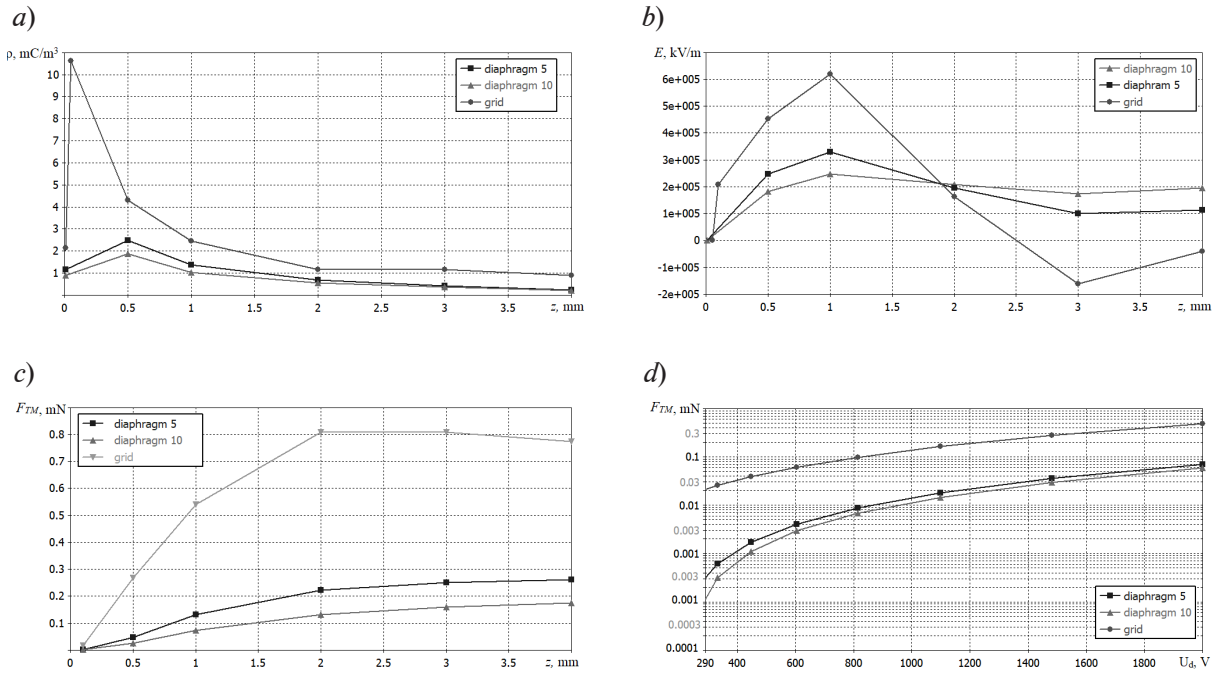


Fig. 4. Numerical calculations for distributions of space charge density (*a*), electric field (*b*) and resultant mechanical force $F_{TM}$ depending on $z$ и $U(d)$ along the coordinate $z$ along the central axis of ion accelerator.
Dependences were obtained for G (*1*), D5 (*2*), and D10 (*3*) models.
The radius of the emission spot is 10 mm; potentials of the first ($\varphi_1$ with $z = 0$), second ($\varphi_2$) and third ($\varphi_3$) electrodes $\varphi_i$, kV: +1.0; −0.2; +0.2, respectively

two solid electrodes in three-electrode models. Fig. 4 shows typical dependences of electronic, physical and mechanical parameters on the coordinates and operating modes in a three-electrode model with a central electrode mounted in the middle. The values of field and charge density along the $z$ axis were calculated for the model with solid electrodes (see Figs. 2 and 3); the mean field and charge density in the transverse plane were calculated for models with the grid and the aperture (see Fig. 4). Figs. 4 and 5 show the functions $E(z)$, $\rho(z)$, and $F_{TM}$ calculated on the axis $z$ without cross-section averaging (this did not produce significant errors).

Comparing the data in Figs. 2, 3, and 4, we can see that the two-stage scheme with an intermediate grid, similar to practical electric propulsion systems, is optimal in forming the ion flux and achieving the greatest mechanical thrust. These electric propulsion systems use volume ionization in a chamber limited by a grid with multiple apertures [6, 10, 11].

Based on the obtained data, we performed computer simulation of three-dimensional multi-electrode sectioned ion accelerators, intended for Hall-effect electric propulsion systems [6, 10, 11]. A preselected multielectrode scheme of an ion accelerator typical for Hall thrusters, was given in the CST software package. In contrast to the two and three-electrode schemes, where zero potential was imposed for all surfaces of the external boundary parallelepiped, an open upper boundary was used here (Fig. 5). The model parameters are given in the caption to the figure. The model is based on a sectional ion accelerator with optimized thrust generation and neutralization. Similar to modern thrusters, neutralization in the given devices was carried out by an electron beam. The shape and size of the electrodes, the potentials applied to them, the size of the emission region, and the magnitude of charged current were selected based on the data obtained (see Figs. 2 and 3).

Similar constructions were calculated for different sizes and voltages of external sources, specific ion masses, current modes. We determined the characteristics of ion and electron trajectories combined in the accelerator and neutralizer. We assessed whether it was possible to combine the given functions, simulating a range of ion and electron

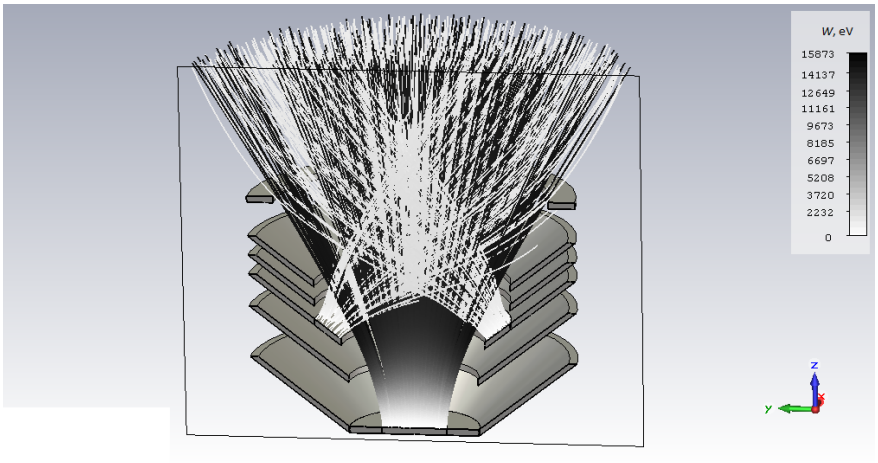


Fig. 5. Schematic model of multi-electrode structure with combined ion and electron trajectories. The ion source is located in the lower part of the model, the electron source is in the middle. The shades of grey correspond to particle energies. Beams intersect near and above the fourth electrode. The potentials of electrodes (from bottom to top electrode) $\varphi_i$, kV: 5.0; -0.5; -1.0; 0.5; 0.0; 0.0. ion and electron currents were equal to 17.5 mA

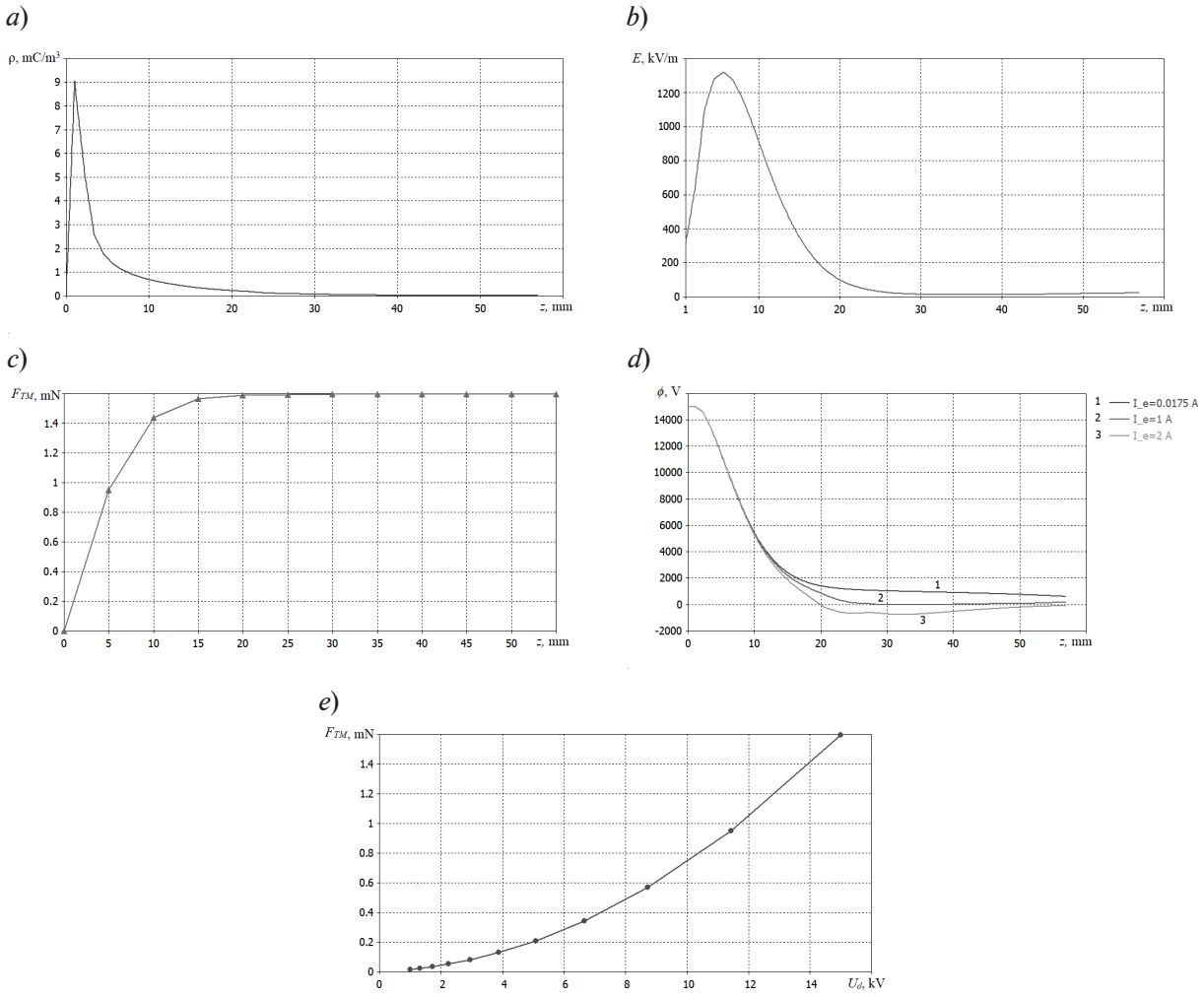


Fig. 6. Numerical calculations for distributions of space charge density (*a*), electric field (*b*), resultant mechanical force $F_{TM}$ (*c*) and potential (*d*) along the coordinate *z* along the central axis of ion accelerator; dependences of resultant mechanical force $F_{TM}$ on the potenial of bottom electrode (*e*); *d* corresponds to electron current $I_e$, A: 0.0175 (*1*), 1.0 (*2*), 2.0 (*3*); *a, b, c, e* correspond to ion current $I_i$ = 17.5 mA

processes as a single process and creating a virtual electronic cathode.

Fig. 5 shows one of the multi-electrode schemes considered with combined ion and electron trajectories. The electron neutralizer of accelerated cations in this example was based on the principle of embedded beams and a virtual cathode, which is fundamentally similar to an plasma ion Hall thrusters but does not require magnetic sources. This should allow to reduce mass, dimensions and energy consumption.

Fig. 6 shows typical dependences of electron, physical and mechanical parameters on the coordinates and operation modes in the multi-electrode model shown in Fig. 5.

Changing the geometric parameters and potentials of electrodes of the model shown in Fig. 5 in a small range, we optimized the ion flux, electron, physical and power characteristics. In particular, we determined the conditions when the electron beam generates an effective potential well for acceleration and capture of ions. Varying the electron current changed the depth of the potential well trapping the ions. Fig. 6, *d* shows acceleration and neutralizion of the ion flux by space charge of electrons. Varying the electron current over a wide range (17.5 mA, 1.0, and 2.0 A) changed the potential in the region $z > 13$ mm, improving focusing and neutralization of the ion flux.

## Conclusion

The CST package was used to construct an analytical electrodynamic algorithm combined with computer simulation of the electromagnetic field and trajectories of charged particles. The algorithm operates by generating mechanical thrust in ion accelerators due to Coulomb interaction of ions moving in vacuum with bound charges on polarized surfaces of the structural elements of the accelerator chamber.

We have considered several models of electrostatic ion accelerators by analytical calculations and computer simulation (using the given package). We have obtained the coordinate dependences of numerical parameters, including the distribution of mechanical forces, potential and field, charge density and current, particle velocity in the accelerating gap. Analysis of the data confirmed that the approaches proposed had satisfactory accuracy and consistency.

The package developed provides a wide range of tools for studying physical phenomena and processes in ionic and plasma ion sources, accelerators and neutralizers for electric propulsion, allowing to assess the designs and parameters of novel devices, comparing different propellants.

The approach presented and the algorithm we have constructed based on this approach may offer potential methods for optimizing newly constructed devices, in particular, by comparing the physical processes for different propellants.

## REFERENCES


1. **Forrester T.A.,** Large ion beams: fundamentals of generation and propagation, Wiley-VCH, Weinheim, Germany, 1988.

2. **Aston G.,** High efficiency ion beam accelerator system, Review of Scientific Instruments. 52 (9) (1981) 1325 − 1327.

3. **Lebedev A.H., Shalnov A.V.,** Osnovy fiziki i tekhniki uskoriteley [Basic foundations of accelerators, Physics and techniques], Energoatomizdat Publisher, Moscow, 1991 (in Russian).

4. **Chao A.W., Tigner M.,** Handbook of accelerator physics and engineering, World Scientific Publishing, London, 1999.

5. **Morozov A.I.,** Plazmennyye uskoriteli i ionnyye inzhektory [Plasma accelerators and ion injectors], Nauka, Moscow, 1984 (in Russian).

6. **Gorshkov O.A., Muravlev V.A., Shagayda A.A.,** Khollovskiye i ionnyye plazmennyye dvigateli dlya kosmicheskikh apparatov [Hall and plasma ion thrusters for spacecrafts], Ed. by Koroteyev A.S., Mashinostroyeniye, Moscow, 2008 (in Russian).

7. **Gusev Yu.G., Pilnikov A.V.,** The electric propulsion role and place within the Russian Space Program, Trudy MAI (Network scientific periodic publication) (60) (2012) 1−20. Access Mode: www.mai.ru/science/trudy/.

8. **Mazouffre S.,** Electric propulsion for satellites and spacecraft: established technologies and novel approaches, Plasma Sources Sci. Technol. 25 (3) (2016) 033002.

9. **Levchenko I., Xu S., Teel G., et al.,** Recent progress and perspectives of space electric propulsion systems based on smart nanomaterials, Nature Communications. 9 (4) (2018) 879.

10. **Goebel D.M., Katz I.,** Fundamentals of electric propulsion ion and Hall thrusters, John Wiley & Sons, Hoboken, New Jersey, USA Ch. 1, 6 and 7 (2008) 1−13, 243−389.

11. **Kaufman H.R.** Technology of electron-bombardment ion thrusters, In the book: Advances in electronics and electron physics. Vol. 36. Ed. by L. Marton, Academic Press, New York (1975) 265–373.

12. **Charles C.,** Plasmas for spacecraft propulsion, J. Phys. D: Applied Phys. 42 (16) (2009) 163001.

13. **Cusson S.E., Dale E.T., Jorns B.A., Gallimore A.D.,** Acceleration region dynamics in a magnetically shielded Hall thruster, Physics of Plasmas, 26 (2) (2019) 023506.

14. **Gopanchuk V.V., Potapenko M.Yu.,** Hall effect thrusters for small-sized spacecrafts, IKBFU's Vestnik. (4) (2012) 60–67.

15. **Favorskiy O.N., Fishgoyt V.V., Yantovskiy Ye.I.,** Osnovy teorii kosmicheskikh elektroreaktivnykh dvigatelnykh ustanovok [Foundations of Hall effect thrusters for spacecrafts], Vysshaya Shkola Publishing, Moscow, 1978.

16. **Hassan A., Elsaftawy A., Zakhary S.G.,** Analytical studies of the plasma extraction electrodes and ion beam formation, Nuclear Instruments and Methods in Physics Research, A. 586 (2) (2008) 148–152.

17. **Kalentev O., Matyash K., Duras J., et al.,** Electrostatic ion thrusters – towards predictive modeling, Contributions to Plasma Physics. 54(2) (2014) 235–248.

18. **Lovtsov A.S., Kravchenko D.A.,** Kinetic simulation of plasma in ion thruster discharge chamber. Comparison with experimental data, Procedia Engineering. 185 (2017) 326–331.

19. **Peng X., Keefert D., Ruytent W.M.,** Plasma particle simulation of electrostatic ion thrusters, Journal of Propulsion and Power. 8 (2) (1992) 361–366.20. **Kurushin A.** Basic course of design of microwave devices using CST Studio Suite, One-Book, Moscow, 2014. 433 p.

21. **Kurushin A.A., Plastikov A.N.,** Proyektirovaniye SVCh ustroystv v srede CST Microwave Studio [Design of microwave devices in CST Microwave Studio], MEI Press, 2011.

22. **Zandberg E.Ya.,** Surface-ionization detection of particles (Review), Technical Physics. 40 (1995) 865–890.

23. **Blashenkov N.M., Lavrent'ev G.Ya.,** Surface-ionization field mass-spectrometry studies of nonequilibrium surface ionization, Phys. Usp. 50 (1) (2007) 53–78.

24. **Tsybin O.Yu., Tsybin Yu.O., Hakansson P.,** Laser or/and electron beam activated desorption of ions: a comparative study, In: Desorption 2004, Papers of 10th International Conference, Saint Petersburg (2004) 61.

25. **Tsybin O.Y., Makarov S.B., Ostapenko O.N.,** Jet engine with electromagnetic field excitation of expendable solid-state material, Acta Astronautica. 129 (December) (2016) 211–213.

*Received 20.01.2020, accepted 08.03.2020.*

## THE AUTHORS

**DYUBO Dmitry B.**
*Peter the Great St. Petersburg Polytechnic University*
29 Politechnicheskaya St., St. Petersburg, 195251, Russian Federation
doobinator@rambler.ru

**TSYBIN Oleg Yu.**
*Peter the Great St. Petersburg Polytechnic University*
29 Politechnicheskaya St., St. Petersburg, 195251, Russian Federation
otsybin@rphf.spbstu.ru

## СПИСОК ЛИТЕРАТУРЫ

1. **Форрестер Т.А.** Интенсивные ионные пучки. М.: Мир, 1992. 354 с.

2. **Aston G.** High efficiency ion beam accelerator system // Review of Scientific Instruments. 1981. Vol. 52. No. 9. Pp. 1325 –1327.

3. **Лебедев А.Н., Шальнов А.В.** Основы физики и техники ускорителей. 2-е изд., перераб. и доп. М.: Энергоатомиздат, 1991. 528 с.

4. **Chao A.W., Tigner M.** Handbook of accelerator physics and engineering. London: World Scientific Publishing, 1999. 650 p.

5. **Морозов А.И.** Плазменные ускорители и ионные инжекторы. М.: Наука, 1984. 269 с.

6. **Горшков О.А., Муравлев В.А., Шагайда А.А.** Холловские и ионные плазменные двигатели для космических аппаратов.

Под ред. акад. РАН А.С. Коротеева. М.: Машиностроение, 2008. 280 с.

7. **Гусев Ю.Г., Пильников А.В.** Роль и место электроракетных двигателей в Российской космической программе // Труды МАИ (электронный журнал). 2012. Вып. № 60. С. 1–20. Режим доступа: www.mai.ru/science/trudy/.8. **Mazouffre S.** Electric propulsion for satellites and spacecraft: established technologies and novel approaches // Plasma Sources Sci. Technol. 2016. Vol. 25. No. 3. P. 033002.

9. **Levchenko I., Xu S., Teel G., Mariotti D., Walker M.L.R., Keidar M.** Recent progress and perspectives of space electric propulsion systems based on smart nanomaterials // Nature Communications. 2018. Vol. 9. No. 4. P. 879.

10. **Goebel D.M., Katz I.** Fundamentals of electric propulsion ion and Hall thrusters. Hoboken, New Jersey, USA: John Wiley & Sons, 2008. Ch. 1, 6 and 7. Pp. 1–13, 243–389.

11. **Kaufman H.R.** Technology of electron-bombardment ion thrusters // Advances in Electronics and Electron Physics. Vol. 36. Ed. by L. Marton, New York: Academic Press, 1975. Pp. 265–373.

12. **Charles C.** Plasmas for spacecraft propulsion // J. Phys. D: Applied Phys. 2009. Vol. 42. No. 16. P. 163001.

13. **Cusson S.E., Dale E.T., Jorns B.A., Gallimore A.D.** Acceleration region dynamics in a magnetically shielded Hall thruster // Physics of Plasmas. 2019. Vol. 26. No. 2. P. 023506.

14. **Гопанчук В.В., Потапенко** М.Ю. Электрореактивные двигатели для малых космических аппаратов // Вестник Балтийского федерального университета им. И. Канта. 2012. Вып. 4. С. 60– 67.

15. **Фаворский О.Н., Фишгойт В.В.,** Янтовский **Е.И.** Основы теории космических электрореактивных двигательных установок. М.: Высшая школа, 1978. 384 с.

16. **Hassan A., Elsaftawy A., Zakhary S.G.** Analytical studies of the plasma extraction electrodes and ion beam formation // Nuclear Instruments and Methods in Physics Research. A. 2008. Vol. 586. No. 2. Pp. 148–152.

17. **Kalentev O., Matyash K., Duras J., Lüskow K.F., Schneider R., Koch N., Schirra M.** Electrostatic ion thrusters – towards predictive modeling // Contributions to Plasma Physics. 2014. Vol. 54. No. 2. Pp. 235–248.

18. **Lovtsov A.S., Kravchenko D.A.** Kinetic simulation of plasma in ion thruster discharge chamber. Comparison with experimental data // Procedia Engineering. 2017. Vol. 185. Pp. 326– 331.

19. **Peng X., Keefert D., Ruytent W.M.** Plasma particle simulation of electrostatic ion thrusters // Journal of Propulsion and Power. 1992. Vol. 8. No. 2. Pp. 361–366.

20. **Kurushin A.** Basic course of design of microwave devices using CST Studio Suite. Moscow: One-Book, 2014. 433 p.

21. **Курушин А.А., Пластиков А.Н.** Проектирование СВЧ устройств в среде CST Microwave Studio. М.: Изд-во МЭИ, 2011. 155 с.

22. **Зандберг Э.Я.** Поверхностно-ионизационное детектирование частиц (Обзор) // Журнал технической физики. 1995. Т. 65. № 9. С. 1–38.

23. **Блашенков Н.М., Лаврентьев** Г.Я. Исследование неравновесной поверхностной ионизации методом полевой поверхностно-ионизационной масс-спектрометрии // Успехи физических наук. 2007. Т. 177. № 1. С. 59–85.

24. **Tsybin O.Yu., Tsybin Yu.O., Hakansson P.** Laser or/and electron beam activated desorption of ions: a comparative study //Desorption 2004, Papers of 10th International Conference. Saint Petersburg, 2004. P. 61.

25. **Tsybin O.Y., Makarov S.B., Ostapenko O.N.** Jet engine with electromagnetic field excitation of expendable solid-state material // Acta Astronautica. 2016. Vol. 129. December. Pp. 211–213.

*Статья поступила в редакцию 20.01.2020, принята к публикации 08.03.2020.*

## СВЕДЕНИЯ ОБ АВТОРАХ

**ДЮБО** Дмитрий Борисович — *аспирант Высшей инженерно-физической школы Санкт-Петербургского политехнического университета Петра Великого.*
195251, Российская Федерация, г. Санкт-Петербург, Политехническая ул., 29
doobinator@rambler.ru

**ЦЫБИН** Олег Юрьевич — *доктор физико-математических наук, профессор Высшей инженерно-физической школы Санкт-Петербургского политехнического университета Петра Великого.*
195251 Российская Федерация, г. Санкт-Петербург, Политехническая ул., 29
otsybin@rphf.spbstu.ru